

CLASSIFICATION OF TIGHT CONTACT STRUCTURES ON SOME SEIFERT FIBERED MANIFOLDS

TANUSHREE SHAH

ABSTRACT. We classify tight contact structures with zero Giroux torsion on some Seifert-fibered manifolds with four exceptional fibers. We get the lower bound by constructing contact structures using Legendrian surgery. We use convex surface theory to obtain the upper bound.

1. INTRODUCTION

Contact geometry has been central to many advances in low-dimensional topology. For instance, it played a key role in Kronheimer and Mrowka's proof that all non-trivial knots satisfy property P (where non-trivial surgery yields a manifold with a non-trivial fundamental group) [32]. It also underpinned Ozsváth and Szabó's results showing that the unknot, trefoil, and figure-eight knots are uniquely determined by Dehn surgery [2, 37, 38], among other applications. Martinet proved in [28] that every closed, oriented 3-manifold admits a contact structure, prompting the study and classification on a 3-manifold. Bennequin divided the class of contact structures on a 3-manifold into overtwisted and tight in [1]. The overtwisted ones are in a 1-1 correspondence with homotopy classes of tangent planes on a 3-manifold, proved by Eliashberg in [3], establishing a link to the topology of the manifold.

The emphasis shifted to tight contact structures, which turned out to be far more nuanced. Etnyre and Honda established the non-existence of tight contact structures on certain Seifert fibered manifolds [9], though their existence remains an open problem in many cases. Classification efforts, when existence is known, primarily target prime atoroidal manifolds, as tight structures respect the connected sum decomposition of 3-manifolds, while essential tori can generate infinitely many non-isotopic tight structures. Consequently, initial classifications were often restricted to atoroidal manifolds. Tight contact structures have been classified on S^3 [5], lens spaces [21], and most Seifert fibered spaces with three exceptional fibers [15, 14, 29, 32].

The focus on toroidal manifold came with the classification of tight structures on 3-torus, by Kanda [33] and Giroux [18] (independently) using the theory of characteristic foliations and convex surfaces. Recently, Simone used twisted Heegaard Floer contact invariant to classify tight structures on some toroidal plumbed 3-manifolds [30].

We build on the results above to classify tight contact structures on some toroidal Seifert fibered manifolds with four exceptional fibers with zero Giroux torsion. For the Seifert fibered manifold $M(g, e_0; p_1/q_1, \dots, p_4/q_4)$, where g is the genus of the base surface B , and $e_0 \in \mathbb{Z}$, $\frac{p_i}{q_i} \in (0, 1) \cap \mathbb{Q}$.

We denote the continued fraction expansion of $-\frac{q_i}{p_i}$ by $[a_0^i, a_1^i, \dots, a_{m_i}^i]$ with all $a_i < -1$ integers. The surgery diagram corresponding to $M(0, e_0; p_1/q_1, \dots, p_4/q_4)$ is shown in the Figure 22.

We first look at an example case in detail before proving the general result. We look at the tight contact structures on $M(0, -4; 1/2, 1/2, 1/2, 1/2)$. Once we have calculated the tight contact structures on this example case, it is computationally easy to generalise to manifolds $M = M(e_0, 0; p_1/q_1, p_2/q_2, p_3/q_3, p_4/q_4)$ with $e_0(M) \leq -4$.

Theorem 1. *Let $M = M(e_0, 0; p_1/q_1, p_2/q_2, p_3/q_3, p_4/q_4)$ where $e_0 \leq -4$ and $\frac{p_i}{q_i} \in (0, 1) \cap \mathbb{Q}$ and $\gcd(p_i, q_i) = 1$. On M there are exactly $|(e_0(M) + 1)\prod_{i=1}^4 \prod_{j=1}^{m_i} (a_j^i + 1)|$ tight contact structures with zero Giroux torsion up to contact isotopy. All of these can be constructed by Legendrian -1 surgery and hence are Stein fillable. For each $n \in \mathbb{Z}$ there exists at least one tight contact structure with n -Giroux torsion on M . These tight contact structures are not weakly fillable.*

We start by constructing tight contact structures with zero Giroux torsion by Legendrian surgery to get a lower bound on the number of tight contact structures. These tight contact structures might be isotopic. To distinguish non isotopic contact structures we use Lisca-Matić's result in [26] which uses Chern numbers and Stein structures. To get the upper bound on the number of tight contact structures we use convex surface theory for which we decompose our manifold in 4 solid tori, toric annulus, and 2 circle bundle over {pair of pants} as shown in Figure 4. We start by maximizing the twisting numbers of the exceptional fibers by attaching bypasses. Then we use Honda's classification of tight contact structures on each of the pieces [22, 21]. We then glue these pieces together to construct M . It is possible to get an overtwisted contact structure when we glue two pieces with tight contact structures; we identify and discard such a combination. We look at the dividing curves on the convex surfaces we glue together to find overtwisted disks. Amongst the remaining combinations, we need to identify the isotopic ones from the others. We use relative Euler class [8] to identify non isotopic tight contact structures.

In Section 2 we briefly look at the methods we use to get our lower and upper bound. Then we look at a couple of classification theorems that we use to classify tight contact structures on our Seifert fiberd manifolds. We give the proof of Theorem 1, in a special case in detail for better understanding and then in full generality in Section 3.

It came to the author's notice 6 months before submission that Elif Medetogullari had similar results which were never published.

2. PRELIMINARIES

We expect the reader to be familiar with convex surface theory and contact surgery at the level of [21] and [7]. We will only consider positively co-oriented contact structures, that is, we consider contact structures which satisfy the condition $\alpha \wedge d\alpha > 0$. We recall a few theorems that we use in our proof here.

A contact manifold M is called *holomorphically fillable* if it is the oriented boundary of a compact Stein surface. It is proved by Eliashberg and Gromov that holomorphically fillable structures are tight [6].

Theorem 2. (*Eliashberg*) [19, Theorem 1.3] *If (M', ξ') is a contact manifold, obtained from a holomorphically fillable contact manifold (M, ξ) by Legendrian surgery then (M', ξ') is holomorphically fillable.*

It is proved by Eliashberg in [4] that S^3 with its standard contact structure is holomorphically fillable. Using Theorem 2 we can construct tight contact structures by Legendrian surgery on knots in S^3 with standard contact structure. The following theorem determines when two such tight contact structures are isotopic.

Theorem 3. [25, Theorem 1.2] *Let X be a smooth 4-manifold with a boundary. Suppose J_1 and J_2 are two Stein structures with boundary on X . Let $c(J)$ be the Chern class of the Stein structure J . If the induced contact structures on ∂X are isotopic, then $c(J_1) = c(J_2)$.*

Now we will state some classification results that we use to get the upper bound on the number of tight contact structures on Seifert fibered manifolds. One uses convex surface theory to obtain these results. We refer the reader to [17, 21, 22] for the basics of convex surface theory. Now we set notations as follows. Let M be a 3-manifold with tight contact structures ξ . Let Σ denote embedded (either closed or has Legendrian boundary) oriented surface in M . We denote the set of dividing curves on Σ by Γ_Σ . The term *sign configuration* on a convex surface means the signs of the regions in the complement of dividing curves. Notice that when we say dividing set we mean the dividing curves and the sign configuration on Σ . Let T^2 be a minimal convex torus in standard form. The term minimal is used here to denote that the convex torus has 2 dividing curves. Throughout the paper we will decompose and attach bypasses along minimal convex torus only and so we will omit the word minimal. We denote the slope of its dividing curves by s or $s(T^2)$ when we want to specify the torus and we call it the slope of the torus. Say we have a 3-manifold M with a convex torus as its boundary. By boundary slope, we refer to the slope of the dividing curves on the boundary torus and denote it by $s(\partial M)$. If our manifold has multiple boundary tori, we index them by $\partial(M)_i$ and denote the slopes by $s(\partial(M)_i)$. The slope of the Legendrian ruling is denoted by r . Let $\gamma \in M$ be a Legendrian curve. We denote the twisting number of a curve γ by $t(\gamma)$. and the standard tubular neighborhood of γ by $N(\gamma)$.

Here we state some results that we use to get the upper bound on the number of tight contact structures. Eliashberg gave the classification of tight contact structures on the 3-ball B^3 .

Theorem 4. [5, Theorem 2.1.3] *Two tight contact structures on the ball B^3 which coincide at ∂B^3 are isotopic relative to ∂B^3 .*

Now let us look at some classification results on $S^1 \times D^2$ and on $T^2 \times I$ which will be used in the classification of tight contact structures on Seifert fibered manifolds.

First, we establish some notations. Let $\frac{p_i}{q_i} \in (0, 1) \cap \mathbb{Q}$ and $(p, q) = 1$ we have the following unique continued fraction expansion:

$$-\frac{q}{p} = a_0 - \frac{1}{a_1 - \frac{1}{a_2 \cdots - \frac{1}{a_k}}},$$

with all $a_i < -1$ integers. We identify $-\frac{q_i}{p_i}$ with $[a_0, \dots, a_k]$.

Theorem 5. [21, Theorem 2.3] *Consider the tight contact structures on $S^1 \times D^2$ with convex boundary T^2 , for which $\#\Gamma_{T^2} = 2$ and $s(T^2) = -\frac{q}{p}$. There exist exactly $|(a_0 + 1)(a_1 + 1) \cdots (a_{k-1} + 1)(a_k)|$ tight contact structures on $S^1 \times D^2$ with this boundary condition, up to isotopy fixing T^2 .*

Now let us look at tight contact structures on $T^2 \times I$. We denote the slope of dividing curves on $T^2 \times \{0\}$ by s_0 and the slope of dividing curves on $T^2 \times \{1\}$ by s_1 . We can assume that s_0 is -1 . We write $s_1 = -\frac{q}{p}$.

The statement of classification of tight contact structures on $T^2 \times I$ is in terms of the continued fraction expansion of the boundary slope.

Theorem 6. [21, Theorem 2.2 (2a)] *(Minimally twisting, rotative case) Let Γ_{T_i} , $i = 0, 1$, satisfy $\#\Gamma_{T_i} = 2$ and $s_0 = -1, s_1 = -\frac{q}{p}$. Then $|\pi_0(\text{Tight}^{\min}(T^2 \times I, \Gamma_{T_1} \cup \Gamma_{T_2}))| \leq |(a_0 + 1)(a_1 + 1) \cdots (a_{k-1} + 1)(a_k)|$.*

Theorem 7. [21, Theorem 2.2 (3)] *(Minimally twisting, non-rotative case) Let Γ_{T_i} , $i=0,1$, satisfy $\#\Gamma_{T_i} = 2$ and $s_0 = s_1 = -1$. Then there exists a holonomy map $k : \pi_0(\text{Tight}^{\min}(T^2 \times I, \Gamma_{T_1} \cup \Gamma_{T_2})) \rightarrow \mathbb{Z}$, which is bijective.*

2.1. Giroux torsion. Say we have a contact manifold (M, ξ) . Say $T \in M$ is a convex torus in standard form. We say that (M, ξ) has n -torsion along T if there exists a contact embedding of $(T^2 \times I, \xi_n = \ker(\sin(2n\pi z)dx + \cos(2n\pi z)dy))$ into (M, ξ) , such that $T^2 \times \{t\}$ are isotopic to T . We say that (M, ξ) has n -Giroux torsion if there exists an embedded torus T along which (M, ξ) has n -torsion and there does not exist any embedded torus T' along which (M, ξ) has $(n + 1)$ -torsion [13].

A 3-manifold M is called *irreducible* if every 2-sphere $S^2 \subset M$ bounds a ball $B^3 \subset M$. A 2-sided surface S without S^2 or D^2 components is called *incompressible* if for each disk $D \subset M$ with $D \cap S = \partial D$ there is a disk $D' \subset S$ with $\partial D' = \partial D$. An irreducible manifold M is called *atoroidal* if every incompressible torus in M is ∂ -parallel otherwise, the manifold is called *toroidal*. It is proved by Honda, Kazez, and Matić:

Theorem 8. [24, Theorem 0.2] *Let M be an oriented, closed, connected, toroidal irreducible 3-manifold that contains an incompressible torus. Then M carries \mathbb{Z} many isotopy classes of tight contact structures.*

The converse was later proved by Colin, Giroux, and Honda:

Theorem 9. [2, Theorem 0.2] *Every closed, oriented, atoroidal 3-manifold carries a finite number of tight contact structures up to isotopy.*

This tells us that the only source of \mathbb{Z} many tight contact structures in a closed, connected, oriented 3-manifold is an incompressible torus. The proofs of Theorem 8 and Theorem 9 tell us that these \mathbb{Z} many tight contact structures occur in a neighborhood, $T^2 \times I$, of the incompressible torus. There are \mathbb{Z} many non-isotopic tight contact structures on this $T^2 \times I$ coming from Giroux n -torsion.

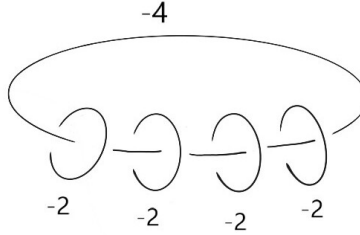


FIGURE 1. Surgery description of the Seifert manifold.

3. TIGHT STRUCTURES ON SEIFERT MANIFOLDS

In this Section, we will be giving the proof of Theorem 1, first in a special case and then in full generality. For details about the construction of Seifert fibered manifolds look at [20]. We first look at a specific example of a Seifert fibered 3-manifold before proving it in full generality.

3.1. Example case of Theorem 1.

Theorem (Special case of Theorem 1). *There are three tight contact structures on $M(0, -4; 1/2, 1/2, 1/2, 1/2)$ modulo Giroux torsion up to contact isotopy. All three of them are Stein fillable. For each $n \in \mathbb{Z}$ there exists at least one tight contact structure with n -Giroux torsion on M up to contact isotopy. These tight contact structures are not weakly fillable.*

Proof. To construct this manifold we follow the method shown in [20]. We start with the surface S^2 . Let X be S^2 with the interior of four disks removed and M' be the circle bundle over X .

Identify each boundary component of $B' \times S^1$ with $\mathbb{R}^2/\mathbb{Z}^2$ by choosing $(1, 0)^T$ to be the direction given by $-\partial(B' \times S^1)$ and $(0, 1)^T$ to be the direction given by the S^1 -fiber. Let V_i 's be the attaching solid tori. We identify ∂V_i with $\mathbb{R}^2/\mathbb{Z}^2$ by choosing $(1, 0)^T$ as the meridional direction and $(0, 1)^T$ as the longitudinal direction. The attaching maps $A_i : \partial V_i \rightarrow -\partial M'$ are given by $\begin{pmatrix} 2 & -1 \\ 1 & 0 \end{pmatrix}$.

The surgery representation of this manifold M is shown on the left-hand side in Figure 1. We perform four (-1) Rolfsen twists to get the surgery diagram on the right in Figure 1. The Legendrian representation of an unknot with surgery coefficient -2 has Thurston-Bennequin number -1 and hence the rotation number is 0. This gives a unique Legendrian representation, for the four -2 framed unknots as shown in Figure 2. For the unknot with surgery coefficient -4 , the Legendrian realization has Thurston-Bennequin number -3 , and hence the rotation number can be $-2, 0$, or 2 . The corresponding Legendrian realizations are shown in Figure 3. Since the rotation numbers of these three Legendrian realizations are different, the Chern numbers of the corresponding Stein structures are different [26], hence, the three contact structures are non-isotopic. Since they are Stein fillable (using Lemma 2) they have zero Giroux torsion [10]. This tells us that there are at least three tight contact structures on M with zero Giroux torsion up to contact isotopy.

3.1.1. *Upper bound.* The Seifert fibered 3-manifold with four exceptional fibers, $M(0, -4; 1/2, 1/2, 1/2, 1/2)$ has an incompressible torus. We would like to count the tight contact structures modulo this \mathbb{Z} many tight contact structures. Consider a $T^2 \times I$ neighborhood of one of the incompressible tori. We

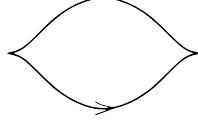


FIGURE 2. Legendrian realization of unknot with Thurston-Bennequin number -1.

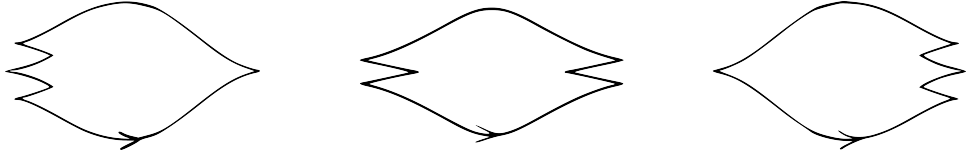


FIGURE 3. Legendrian realizations of the unknot with Thurston-Bennequin number -3.

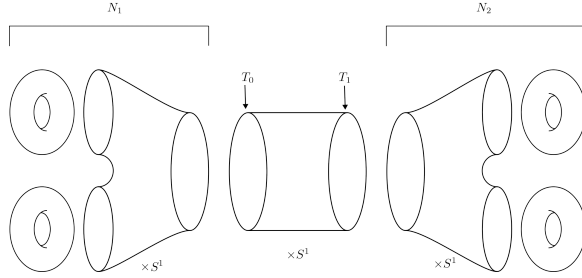


FIGURE 4. Decomposition of a Seifert fibered 3-manifold with four exceptional fibers.

cut along T_0 and T_1 to decompose our manifold in three pieces, one of which is $T^2 \times I$. The other two pieces are denoted by N_1 and N_2 . As shown in Figure 4 each N_i can be decomposed in $\{\text{pair of pants}\} \times S^1$ and two solid tori.

Let us start by looking at one of these pieces, say N_1 . We denote the $\{\text{pair of pants}\} \times S^1$ by $\Sigma \times S^1$ and the two solid tori by V_1, V_2 . There are three boundary components of $\Sigma \times S^1$, which we denote by $\partial(\Sigma \times S^1)_i$, where $\partial(\Sigma \times S^1)_i$ for $i = 1, 2$ corresponds to the torus ∂V_i for $i = 1, 2$ and $\partial(\Sigma \times S^1)_3$ is glued to the $T^2 \times I$. Note that $\partial(\Sigma \times S^1)_3$ is the same as ∂N_1 . We denote the two singular fibers by F_1 and F_2 and their twisting numbers by n_1 and n_2 . Since V_1 and V_2 are standard neighborhoods of F_1 and F_2 . Assume that these are simultaneously isotoped to Legendrian curves and further isotoped so that their twisting number is negative. The slope of the dividing curves (Example 1.4.12 in [31]) on ∂V_i is $\frac{1}{n_i}$. Using the construction from [20], the two attaching maps $A_i : \partial V_i \rightarrow -\partial(\Sigma \times S^1)_i$ are given by $\begin{pmatrix} 2 & -1 \\ 1 & 0 \end{pmatrix}$ for $i = 1, 2$. Note that the slope of dividing curves on $\partial(\Sigma \times S^1)$ is not ∞ . Using the flexibility of Legendrian ruling (Corollary 3.6 in [21]) we may assume that the Legendrian ruling slope of $\partial(\Sigma \times S^1)_i$ for $i = 1, 2, 3$ is infinite.

3.1.2. *Maximising twisting numbers.* We use the same methods to maximize the twisting number as illustrated in [16]. For $i = 1, 2$ we have $A_i.(n_i, 1)^T = (2n_i - 1, n_i)$. We denote the slope of the dividing curve on $-\partial(\Sigma \times S^1)_i$ by $s(\partial(\Sigma \times S^1)_i) = \frac{n_i}{2n_i - 1}$.

Lemma 10. *We can increase the twisting numbers n_1 and n_2 up to 0.*

Proof. Consider an annulus $I \times S^1$ in M from $\partial(\Sigma \times S^1)_1$ to $\partial(\Sigma \times S^1)_2$ such that its boundary consists of Legendrian ruling curves on the tori. The boundary of this annulus intersects the dividing curves in $2(2n_i - 1)$ points respectively.

If $n_1 \neq n_2$ then, due to the imbalance principle ([23]) there exists a bypass along a Legendrian ruling curve on either of the boundaries. Note that $A_i^{-1} = \begin{pmatrix} 0 & 1 \\ -1 & 2 \end{pmatrix}$ and hence the Legendrian ruling has slope 2 on ∂V_i . Using the twist number Lemma we can attach a bypass and thicken V_i to V'_i increasing the twisting number as long as $n_i < 0$. We can apply the imbalance principle till $n_1 = n_2$. Since $n_1 = n_2$ there are an equal number of bypasses on both ends. We attach any remaining bypasses, if any, on either of the boundaries. Once you attach all the bypasses, there will be no boundary parallel dividing curves and, hence all the dividing curves will run from one boundary component to the other.

Now, we can assume that $n_1 = n_2$ and there is no bypass on the annulus $A = I \times S^1$ in M from $\partial(\Sigma \times S^1)_1$ to $\partial(\Sigma \times S^1)_2$. Then we cut $N_1 \setminus (V'_1 \cup V'_2)$ open along A . Note that a neighborhood of $A \cup V'_1 \cup V'_2$ is a piecewise smooth solid torus with four edges. We use the edge rounding Lemma (Lemma 3.11, [21]) to smoothen these four edges. Since each rounding changes the slope by an amount of $-\frac{1}{4} \frac{1}{2n_1 - 1}$, the slope of the diving curves on the boundary torus is

$$s(\partial(\Sigma \times S^1)_1) + s(\partial(\Sigma \times S^1)_2) - 4\left(\frac{1}{4} \frac{1}{2n_1 - 1}\right) \\ \frac{n_1}{2n_1 - 1} + \frac{n_1}{2n_1 - 1} - \frac{1}{2n_1 - 1} = 1.$$

This boundary torus is isotopic to ∂N_1 and identified with $\mathbb{R}^2/\mathbb{Z}^2$ in the same way as ∂N_1 . Hence the slope of the dividing curves on boundary torus $-\partial N_1$ is -1 .

Now take an annulus $I \times S^1$ from $\partial(\Sigma \times S^1)_1$ to ∂N_1 . For $n_1 < 0$ we have $2n_1 - 1 < -1$. Hence there exists a bypass by the imbalance principle on V_1 until we increase n_1 up to 0. One can do a similar calculation for n_2 . Hence we can increase n_1 and n_2 until $n_1 = n_2 = 0$. □

3.1.3. *Combining tight contact structures on basic blocks.* We have $n_1 = n_2 = 0$. The slope of the dividing curves on $-\partial N_1$ is -1 , on $\partial(\Sigma \times S^1)_1$ is 0 and on $\partial(\Sigma \times S^1)_2$ is 0. Now we count the number of tight contact structures on $\Sigma \times S^1$ when the slope of the dividing curves on the three boundary tori is $0, 0, -1$. Again consider an annulus $I \times S^1$ from $\partial(\Sigma \times S^1)_1$ to $\partial(\Sigma \times S^1)_2$. Either there exists a bypass on both boundary components or not.

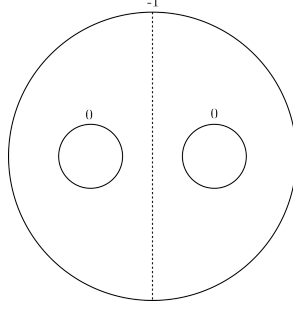


FIGURE 5. Dividing curve on Σ with contact structure ξ_A on $\Sigma \times S^1$.

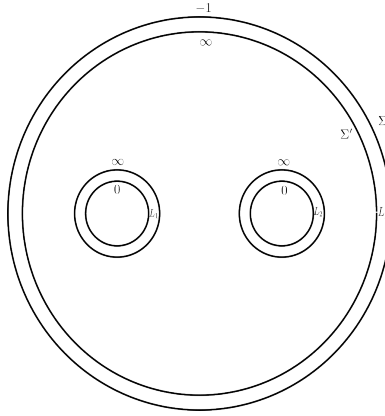


FIGURE 6. Σ and Σ' with their boundary slopes.

Case 1: If no bypass exists then we have the following conditions: According to the classification Lemma 5.1 of Honda [22], $\Sigma \times S^1$ with such boundary slopes has a unique tight contact structure as shown in Figure 5 (Note that we are using the opposite sign convention to Honda's). Call it ξ_A . Using the A_i^{-1} the slope of the dividing curve on the boundary of V_i for $i = 1, 2$ is ∞ . By Proposition 5, there is exactly one tight contact structure on V_i for $i = 1, 2$. This gives a unique tight contact structure on N_1 .

Case 2: If there is a bypass then the cutting and rounding construction (see edge rounding in [23]) gives a torus of infinite slope after a bypass attachment. Then Honda's classification of tight contact structures on $\Sigma \times S^1$ (Lemma 5.1, [22]) asserts that there exists a unique factorisation $\Sigma \times S^1 = \Sigma' \times S^1 \cup L_1 \cup L_2 \cup L_3$, where the L_i are $T^2 \times I$ with minimal twisting and all components of the boundary of $\Sigma' \times S^1$, denoted by $\partial(\Sigma' \times S^1)_i$, have dividing curves of ∞ slope. Figure 6 shows Σ and Σ' with their boundary slopes. Here we fix Σ to be $\Sigma \times \{0\}$ and Σ' to be $\Sigma' \times \{0\}$.

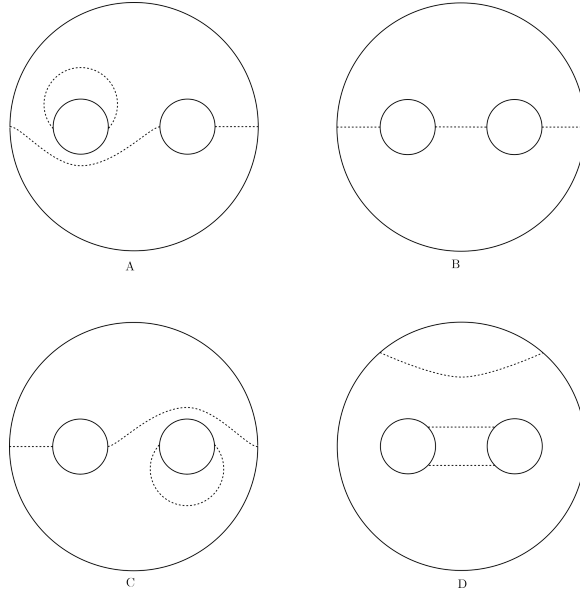


FIGURE 7. Possible dividing curves on pair of pants.

Let us start by looking at the tight contact structures on $\Sigma' \times S^1$ and then add in the L_i to get the tight contact structures on $\Sigma \times S^1$. Each boundary component of Σ' intersects the dividing set of the corresponding torus twice.

Lemma 11. *Dividing curves on Σ' either connect boundary components in pairs as in Figure 7 B, or we have one boundary parallel dividing curve on $\partial(\Sigma \times S^1)_3$ and two dividing curves connecting $\partial(\Sigma \times S^1)_1$ to $\partial(\Sigma \times S^1)_2$ as shown in Figure 7 D.*

Proof. We call $\partial(\Sigma \times S^1)_1$ as boundary component one. Similarly for boundary component two. Assume there is a boundary-parallel dividing arc on boundary component one or on boundary component two as shown in Figure 7 A, C. Say the boundary parallel dividing arc is across $\partial(\Sigma \times S^1)_1$. This means there is a bypass along $\partial(\Sigma \times S^1)_1$. After attaching this bypass we can thicken $V_1 \cup L_1$ to get V'_1 . The slope on the boundary of V'_1 is 0 in the basis of $\Sigma' \times S^1$. Hence we have a toric annulus L_1 with boundary slopes 0 and ∞ and an extension of this toric annulus is another toric annulus with boundary slopes ∞ and 0. The slope goes from 0 to ∞ to 0 on V'_1 and hence the contact structures on V'_1 are overtwisted. Similarly, we get an overtwisted contact structure if we have a boundary-parallel dividing arc on boundary component two. The possible dividing curve configurations without boundary-parallel dividing arcs on boundary component one or on boundary component two are of the form described in this Lemma. □

From the result in Lemma 11 we can divide our analysis into two cases, corresponding to Figure 7 B or D. These are two different dividing sets corresponding to different contact structures on $\Sigma \times S^1$. We will first count all the tight contact structures we get corresponding to Figure 7 B. We refer to this analysis as Case 2A. Then we do the same for Figure 7 D and refer to it by Case 2B.

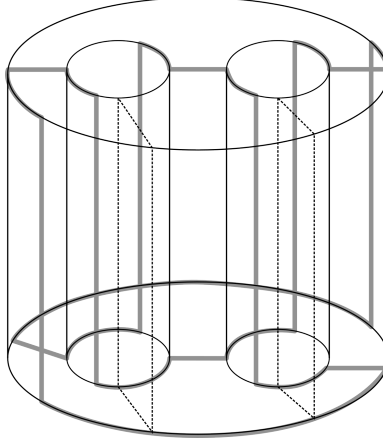


FIGURE 8. Dividing curves on boundary of $\Sigma' \times I$.

Case 2A: Consider the set of dividing curves where each curve on Σ' connects one boundary component to the other as shown in Figure 7 B. The following Lemma is proved by Honda and Etnyre [9]. I restate it for clarity.

Lemma 12. *The two dividing sets given by two different sign configurations in Figure 7 B give a unique contact structure on $\Sigma' \times S^1$.*

Proof. We start by cutting $\Sigma' \times S^1$ along Σ' and then round the edges (see edge rounding in [23]). We get a solid genus-two handlebody. We can arrange the dividing curves on the boundary so that two meridional disks intersect the dividing set exactly twice. (This is shown in Figure 8.) Hence there is a unique dividing curve, separating the two intersection points, on these two disks. We cut along these two disks to get a 3-ball. There is a unique contact structure on this 3-ball with the given restriction to the boundary surface (Theorem 4). Since the dividing curves on the surface, we cut along are determined by our initial configuration of dividing curves, we get a unique contact structure on $\Sigma' \times S^1$. \square

Case 2B: Let us look at the case when one dividing curve goes from $\partial(\Sigma \times S^1)_3$ to itself and two dividing curves go from $\partial(\Sigma \times S^1)_1$ to $\partial(\Sigma \times S^1)_2$ as shown in Figure 7 D. This gives us at most two tight contact structures on $\Sigma \times S^1$ for Case 2B, one for each sign configuration.

We now look at the dividing curves on $\Sigma \times S^1 = \Sigma' \times S^1 \cup L_1 \cup L_2 \cup L_3$. Let $A_i = \Sigma \cap L_i$. For the contact structure on $\Sigma \times S^1$ to be tight the dividing set of A_3 will have two arcs connecting the boundary components. There are two possible configurations depending on the sign of the basic slice L_3 . The dividing set of A_1 and A_2 consists of a boundary parallel arc on the boundary component with dividing curves of the infinite slope. There are two possible configurations depending on the sign of the respective basic slice. This is shown in Figure 12. Again dotted lines represent the dividing curves.

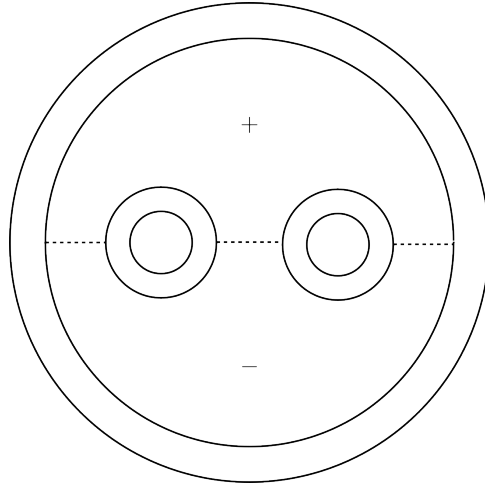


FIGURE 9. Possible dividing set on Σ .

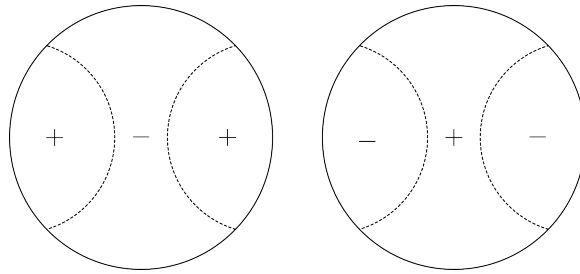


FIGURE 10. Two possibilities of dividing curves on \mathbb{D}^2 with $t(\partial\mathbb{D}) = -2$ [21].

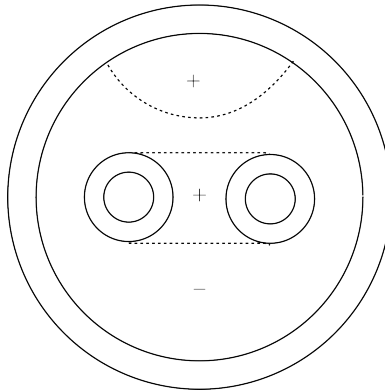


FIGURE 11. Possible dividing set on Σ .

Now let us look at the dividing curves on $\Sigma \times S^1$ separately for Case 2A and Case 2B as we did before.

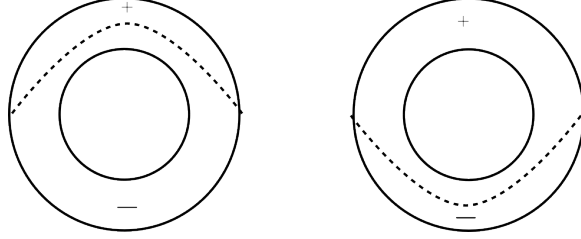


FIGURE 12. Positive (left) and Negative (right) sign configuration of dividing sets on A_2 and A_1 .

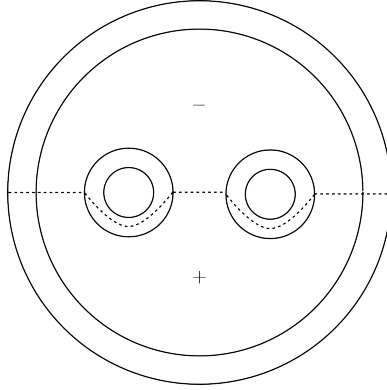


FIGURE 13. Dividing set of ξ_B on Σ .

Case 2A: We fix one sign configuration for the contact structure on $\Sigma' \times S^1$ as shown in Figure 9. This fixes the sign configuration of the contact structure on L_3 . In our case it is positive. We write (\pm, \pm, \pm) to denote that the signs of the basic slices, L_i for $i = 1, 2, 3$ are positive/negative. Now we have a choice of sign for the contact structure on L_1 and L_2 . This gives us four total configurations, given by: $(+, +, +), (-, -, +), (-, +, +), (+, -, +)$. It is proved in [22] (Lemma 5.1, 9th paragraph in the proof) that if all three basic slices have the same sign then we get an overtwisted disk. Hence $(+, +, +)$ corresponds to an overtwisted contact structure on $\Sigma' \times S^1$.

We can have a contact structure with $(-, -, +)$ configuration. This corresponds to one tight contact structure on $\Sigma \times S^1$ with the slopes of the dividing curve on the boundary torus $0, 0, -1$. The dividing set is shown in Figure 13. The tight contact structure on $\Sigma \times S^1$ corresponding to this dividing set on Σ will be denoted by ξ_B . If we had started our Case 2A with the opposite signed configuration, then we would have the dividing set as shown in Figure 14 on Σ . This corresponds to a different tight contact structure because the relative Euler classes are different on $\Sigma \times S^1$. Let us call it $\xi_{B'}$.

Similarly we can have $(-, +, +)$ and $(+, -, +)$ configuration. The dividing sets corresponding to these signed configurations are shown in Figure 15. Each of these corresponds to one tight contact structure on $\Sigma \times S^1$. We denote them by ξ_C and ξ_D . If we had started our Case 2A with the opposite

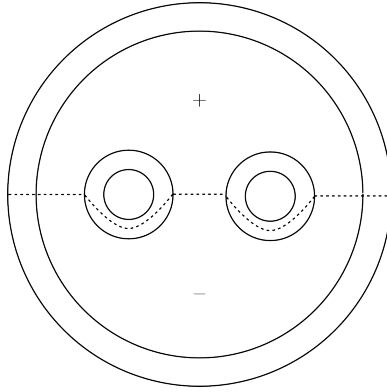


FIGURE 14. Dividing set of $\xi_{B'}$ on Σ .

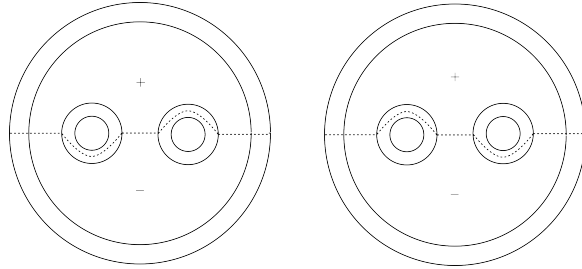


FIGURE 15. Dividing set of ξ_C and ξ_D on Σ .

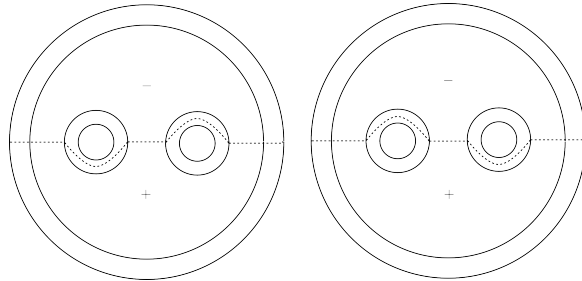


FIGURE 16. Dividing set of $\xi_{C'}$ and $\xi_{D'}$ on Σ .

signed configuration, then we would have the dividing sets shown in Figure 16 on Σ . These correspond to different tight contact structures on $\Sigma \times S^1$. Let us call them $\xi_{C'}$ and $\xi_{D'}$.

Case 2B: We have fixed one sign configuration for $\Sigma' \times S^1$ as shown in Figure 11. This fixes the sign configuration of L_3 . Now we have a choice for sign-on L_1 and L_2 . This gives us four total configurations shown in Figure 17. The case where both the L_1 and L_2 have positive signs yields an overtwisted contact structure. We can see the dividing curves by dotted lines in Figure 17 A. The boundary of the overtwisted disk is outside the disk-bound by these dividing curves. Now consider

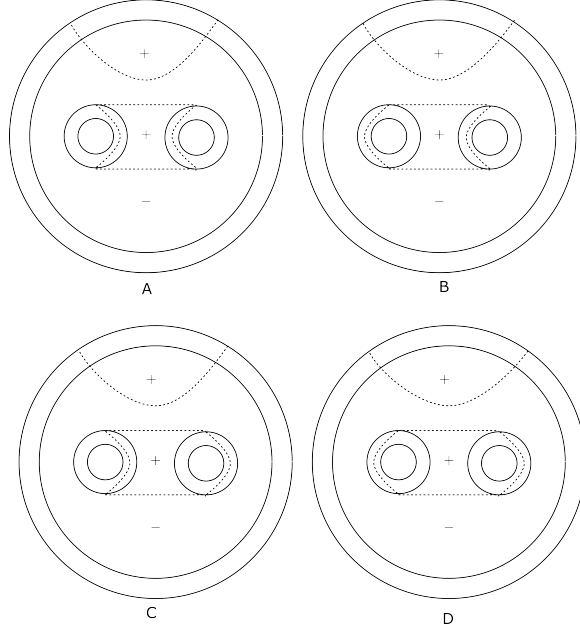


FIGURE 17. Four possible configurations of dividing curves on Σ .

the case when L_1 and L_2 have mixed signs. Then we get a bypass on the L_i with a negative sign as shown in Figure 17 B, C. Say the bypass is on L_1 . We can attach this bypass and thicken our solid torus to get a solid torus with boundary slope 0. Hence we have a toric annulus L_1 with boundary slopes 0 and ∞ and an extension of this toric annulus is another toric annulus with boundary slopes ∞ and 0. Hence we have too much radial twisting in V'_1 and hence the contact structures on V'_1 are overtwisted. Similarly, we get an overtwisted contact structure if we have a boundary-parallel dividing arc on boundary component two. Hence we are left with the case where both L_1 and L_2 have negative signs as shown in Figure 17 D. This contact structure on $\Sigma \times S^1$ is denoted by ξ_E . We would get the opposite signed configuration if we had started Case 2B with the other sign configuration. This will be denoted ξ'_E and it is shown in Figure 18.

We have nine tight contact structures on $\Sigma \times S^1$ denoted by $\xi_A, \xi_B, \xi_{B'}, \xi_C, \xi_{C'}, \xi_D, \xi_{D'}, \xi_E, \xi_{E'}$. There is a unique tight contact structure on each V_i . Let us glue the two $\Sigma \times S^1$ along the toric annulus (refer section 3.1.1). When we are gluing the two $\Sigma \times S^1$ we are gluing using an orientation reversing diffeomorphism so we have to glue them using $T^2 \times I$ with boundary slopes -1 and $+1$. After gluing, we get $\{\text{sphere with four holes}\} \times S^1$, denoted by $X \times S^1$, which we call Y . Let us look at all possible tight contact structures on Y with zero Giroux torsion. Figure 19 shows all possible dividing curve configurations on the sphere with four holes which give potentially tight contact structures with zero Giroux torsion after gluing the two pairs of pants. The tight contact structure on Y we get by gluing two pairs of pants with ξ_E and $\xi_{E'}$ is shown in Figure 20. This contact structure has non-zero Giroux torsion depicted by the dividing curves on the toric annulus. They describe the twisting of contact planes on toric annulus $\times S^1$ from slope 0 to ∞ to 0 to ∞ to 0, to *infy*, which is one full twist. All other combinations of gluing two pairs of pants give us an obvious overtwisted disk in Y .

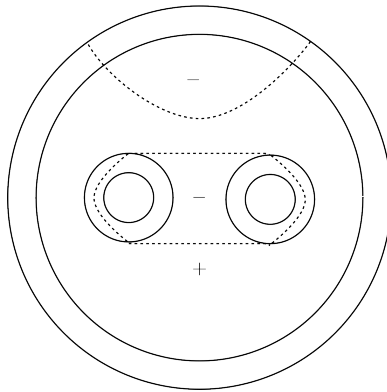


FIGURE 18. Dividing set of $\xi_{E'}$ on Σ .

When we glue the four solid tori to Y with contact structure as determined by the dividing curves in pictures 5, 6, 7, and 8 of Figure 19 we get overtwisted contact structures on $M(0; -1/2, -1/2, -1/2, -1/2)$, indeed in all of these cases, there is a boundary parallel dividing curve, say γ_1 , on the X . There is a boundary parallel torus, say T_1 containing γ_1 . We denote this boundary torus as T_0 and the dividing curve on it as γ_0 . Consider the $T^2 \times [0, 1]$ from T_0 to T_1 . The dividing curves γ_0 and γ_1 have slope zero, hence we have a boundary parallel torus corresponding to every slope in this $T^2 \times I$. So in particular we have a torus with slope $\frac{1}{2}$. Using A_i^{-1} this corresponds to slope zero in the basis of the glued in solid torus. Hence this dividing curve bounds a meridional disk in the solid torus which is our overtwisted disk.

We use the relative Euler class (see Section 4.2 in [21]) to show that pictures 3 and 4 (as shown in Figure 19) yield non-isotopic tight contact structures on Y . We denote the i th tight contact structure in Figure 19 as ξ_i . We have that the relative Euler class $e(\xi_3) = -2$ whereas $e(\xi_4) = 2$. Diagrams 1 and 2 (as shown in Figure 19) can be shown to be equivalent by section changes similarly to those discussed in Section 3.2. So we get at most three potentially tight contact structures on $X \times S^1$.

Since the upper bound and lower bound (which we computed in Section 3.1) both are three, we get that $|\pi_0(\text{Tight}^{min}(M))| = 3$. All of these are Stein fillable, since we get these three contact structures on M by doing a -1 Legendrian surgery on a Legendrian link in (S^3, ξ_{std}) .

Since M is toroidal there are \mathbb{Z} many non-isotopic tight contact structures on M corresponding to integral Giroux torsion. It is proved by Gay in [10] that tight contact structures that are strongly symplectically fillable have no Giroux torsion. Also, it is proved in [11] that a weakly fillable tight contact structure on a rational homology sphere is a strongly fillable contact structure. The Seifert fibered manifold M is a rational homology sphere. Hence the tight contact structures on M with non-zero Giroux torsion are not weakly fillable. \square

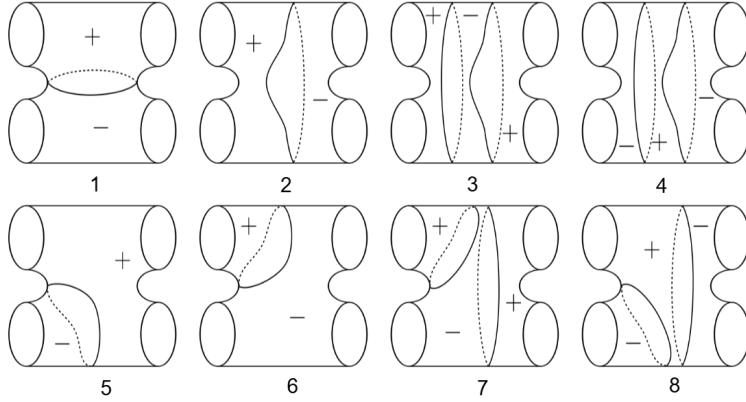


FIGURE 19. Dividing curve configurations on the sphere with four holes representing all possible tight contact structures on Y with zero Giroux torsion.

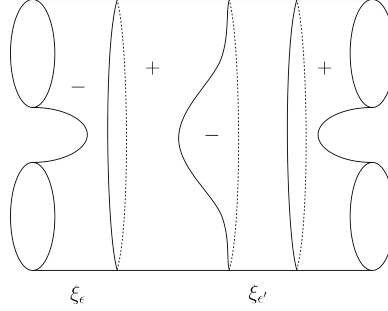


FIGURE 20. Dividing curve configuration showing non-zero Giroux torsion.

3.2. General case. Consider the manifold $M = M(0, e_0; p_1/q_1, \dots, p_4/q_4)$ where $e_0 \leq -4$ and $p_i, q_i \in \mathbb{Z}$ with $e_0 \in \mathbb{Z}$, $\frac{p_i}{q_i} \in (0, 1) \cap \mathbb{Q}$, and $(p_i, q_i) = 1$, $\frac{-q_i}{p_i} = [a_0^i, a_1^i, \dots, a_{m_i}^i]$, where all a_j^i 's are integers, $a_0^i = \lfloor \frac{-q_i}{p_i} \rfloor \leq -1$, and $a_j^i \leq -2$ for $j \geq 1$. We define $p_j^i = -a_j^i p_{j-1}^i - p_{j-2}^i$ for $j = 0, 1, \dots, m_i$ and $p_{-2}^i = -1$ and $p_{-1}^i = 0$. Similarly we define $q_j^i = -a_j^i q_{j-1}^i - q_{j-2}^i$ for $j = 0, 1, \dots, m_i$ and $q_{-2}^i = -1$ and $q_{-1}^i = 0$. The previous example (Section 3.1) we have considered has $e_0(M) = -4$ and $\frac{-q_i}{p_i} = -2$. Once we have calculated the tight contact structures on this example case, it is computationally easy to generalise to the case of all manifolds M with $e_0(M) \leq -4$.

Proof of Theorem 1. To prove this theorem we follow similar methods as we used for our example case (see Section 3.1). We need an additional section change operation to show that some of the potential tight contact structures are isotopic. The operation that Hatcher ([20, Proof of Proposition 4.1]) demonstrates in Figure 4.1, is what we denote as section change, although Hatcher never uses this terminology. Here we briefly describe this operation for the reader's convenience. Since we have a circle bundle $M' \rightarrow B'$ we can choose a section. This choice determines the slope on the boundary of M' . Let's examine how the slopes on the boundary change when we opt for a different section. Say a is an arc with endpoints in $\partial B'$. There is an annulus corresponding to this arc in M' , say A .

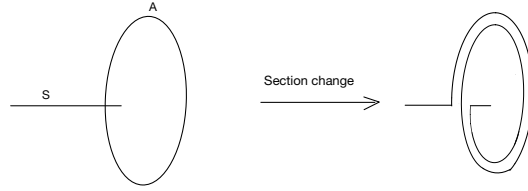


FIGURE 21. Section change to get diffeomorphic Seifert fibered manifold [20]

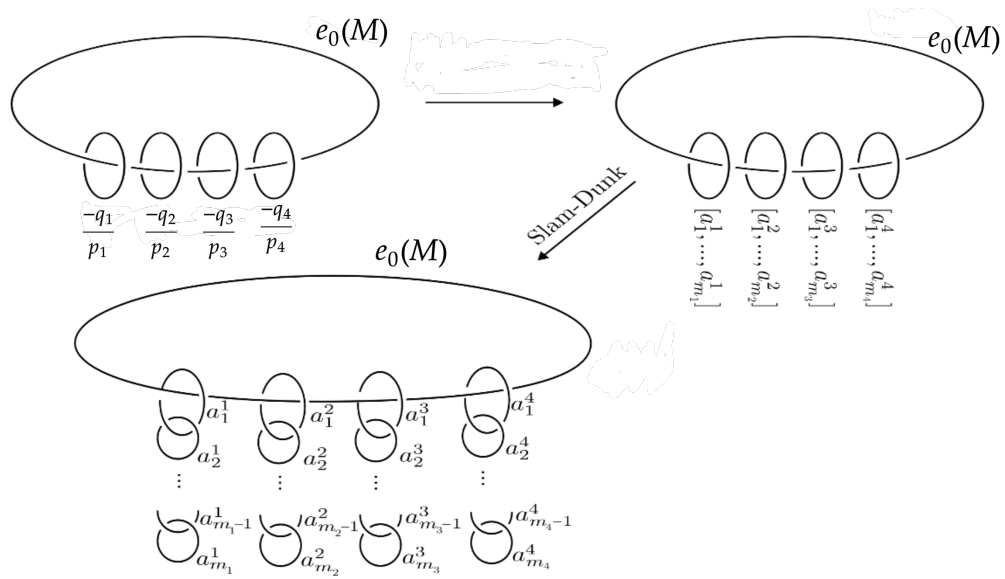


FIGURE 22. Surgery diagram representations of the manifold $M = M(0, e_0; p_1/q_1, \dots, p_4/q_4)$

The new section we choose winds m times around A as it crosses A as illustrated in Figure 21. This effectively adds m to the boundary slope at one end of A and subtracts m from the other boundary slope.

The surgery diagram for the construction of $M = M(0, e_0; p_1/q_1, \dots, p_4/q_4)$ is shown in Figure 22 on top left. We perform Rolfsen twists to get the surgery diagram on the top right. We do a slam dunk operation to obtain the diagram at the bottom. One can refer to [16] for both these operations. The number of Legendrian realisations for each of the unknots is $(a_i^j + 1)$ or $(e_0(M) + 1)$ based on their Thurston-Bennequin and rotation numbers. Then by Theorem 3 there are at least $|(e_0(M) + 1)\prod_{i=1}^4 \prod_{j=1}^{m_i} (a_j^i + 1)|$ tight contact structures with zero Giroux torsion on M up to contact isotopy. This gives a lower bound on the number of tight contact structures on M .

3.2.1. *Upper Bound.* We start with the decomposition of the Seifert fibered manifold as stated previously in the example case. The manifold $M = M(0, e_0; p_1/q_1, \dots, p_4/q_4)$ has incompressible tori. We are going to start by counting tight contact structures with zero Giroux torsion on M .

Using the same construction and notations from the example case as in Figure 4 we have that the two attaching maps $A_i : \partial V_i \rightarrow -\partial(\Sigma \times S^1)_i$ is given by $\begin{pmatrix} p_i & u_i \\ q_i & v_i \end{pmatrix} \in SL_2(\mathbb{Z})$ for $i = 1, 2$ where $u_i = p_{m_i-1}^i$ and $v_i = q_{m_i-1}^i$. Using the flexibility of Legendrian ruling we assume that the ruling slope of $\partial(\Sigma \times S^1)_i$ for $i = 1, 2, 3$ is infinite. Assume that the fibers F_i are simultaneously isotoped to Legendrian curves such that their twisting numbers are particularly negative. For $i = 1, 2$ we have $A_i \cdot (n_i, 1)^T = (n_i p_i + u_i, n_i q_i + v_i)$. We denote the slope of the dividing curve on $-\partial(\Sigma \times S^1)_i$ by $s_i = \frac{n_i q_i + v_i}{n_i p_i + u_i} = \frac{q_i}{p_i} + \frac{1}{p_i(n_i p_i + u_i)}$.

Note that the manifolds, $M = M(0, e_0; p_1/q_1, \dots, p_4/q_4)$, we are working with are L-spaces (see Theorem 1.1 [27]). We look at Seifert fibered manifold $M' = (0; -q_1/p_1, \dots, -q_3/p_3)$ which is an L-space with $e_0 \leq -2$. Any tight contact structures on M' has a Legendrian curve with twisting number -1 in the $\Sigma \times S^1$ (Using Corollary 5.2 from [12]). We call this curve L and its neighborhood V . We can construct M from M' by doing a surgery on a fiber which is not in V . Hence we have a Legendrian curve with twisting number -1 in our manifold M . We can assume that the Legendrian ruling slope on $\partial(\Sigma \times S^1)_i$ for $i = 1, 2$ is ∞ . Take an annulus A_i between ∂V and $\partial(\Sigma \times S^1)_i$ for $i = 1, 2$. There might be some bypasses on $\partial(\Sigma \times S^1)_i$ by the imbalance principle. After attaching these bypasses the slope of the dividing curve on $\partial(\Sigma \times S^1)_i$ is $\lfloor \frac{q_i}{p_i} \rfloor$ for $i = 1, 2$. One can similarly prove that the dividing curve on $\partial(\Sigma \times S^1)_i$ is $\lfloor \frac{q_i}{p_i} \rfloor$ for $i = 3, 4$.

3.2.2. *Combining tight contact structures on the basic blocks.* After we glue the two $\Sigma \times S^1$ across the toric annulus we get $X \times S^1$ which we call Y' . The slope of the dividing curves on the boundary tori of Y' is $\lfloor \frac{q_i}{p_i} \rfloor$ for $i = 1, 2, 3, 4$. We take a suitable diffeomorphism of $X \times S^1$ to normalize the boundary slopes to be $\sum_{i=1}^4 \lfloor \frac{q_i}{p_i} \rfloor = s$ on one of the boundary torus and 0 on the other three boundary tori. This amounts to a section change. We denote this $X \times S^1$ by Y . The number of tight contact structures up to contact isotopy on the manifold before the section change is the same as the number of tight contact structures up to contact isotopy on the manifold after the section change. Since $s \geq 0$ we can decompose Y in a $X \times S^1$ with all four boundary slopes 0 and a toric annulus with boundary slopes 0 and s . This is shown in Figure 23.

There are three tight contact structures with zero Giroux torsion on $X \times S^1$ with all four boundary slopes 0 (as proved in Section 3.1.3). There are $(s + 1)$ tight contact structures on a toric annulus with boundary slopes 0 and s [21]. When we glue this toric annulus on $X \times S^1$, we need the signs of the regions on the boundary to match. There are $3s + 3$ combinations but only $2s + 3$ are possible because the signs of the regions should match at the gluing. So we get an upper bound of $2s + 3$ on the number of potential tight contact structures.

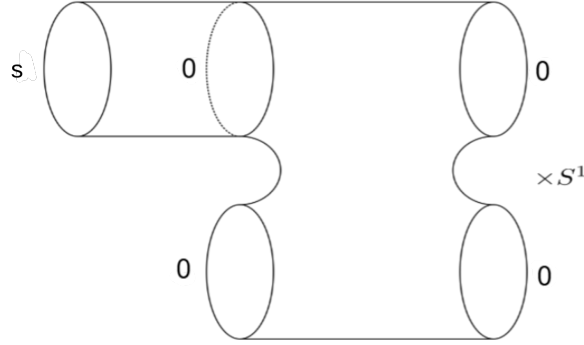
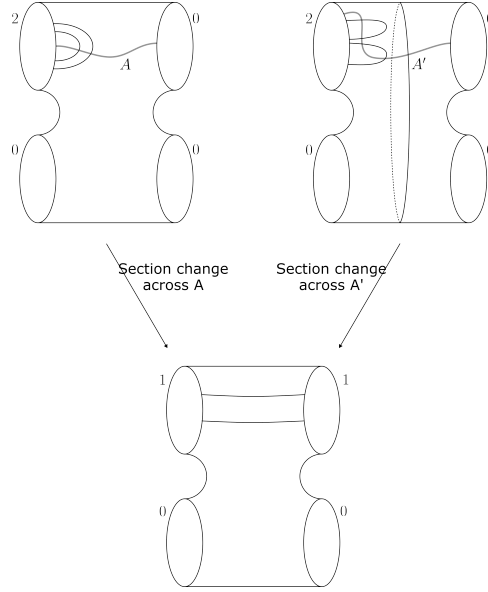


FIGURE 23. Decomposition of Y .

We write the boundary slopes on Y as (s_1, s_2, s_3, s_4) where the slope s_i is $s(\partial Y)_i$. Say that our boundary slopes on Y are $(2, 0, 0, 0)$. We will show that the two dividing curve configurations shown on a X in Figure 24 (top right and top left) represent two different sections (as in Prop. 2.1 in [20]) of the same contact structure on $X \times S^1$. We start with a tight contact structure that has a positive and negative bypass on the boundary component with boundary slope 2. This dividing curve configuration is shown on the top left. Consider an annulus A between boundary component having slopes 2 and 0, as shown in Figure 24. We do the section change (as in Prop. 2.1 in [20]) across annulus A to get Y'' with boundary slopes $(1, 1, 0, 0)$. We obtain the dividing curves on the new section of Y'' as follows: we start with our old section on $X \times S^1$ with boundary slopes $(2, 0, 0, 0)$ and draw the dividing curves on the X as well as on all four boundary tori. Using the construction as in Prop. 2.1 in [20] we draw our new section (with boundary slopes $(1, 1, 0, 0)$) in our old $X \times S^1$ (with boundary slopes $(2, 0, 0, 0)$). We mark all intersections of the dividing curves with the boundary of the new section. Since the new X is embedded in old $X \times S^1$, we start drawing the dividing curve at one of the boundary components with slope 1 and follow through in our new X across the old section. We get the dividing curves connecting the two boundary components with boundary slopes 1. This dividing curve configuration is shown in Figure 24 at the bottom. Next, we look at the dividing curve configuration which has the two same signed bypasses on the boundary component with slope 2 and half a twist across the incompressible torus. This dividing curve configuration is shown on the top right. We do the section change along annulus A' between boundary components having slopes 2 and 0 which goes across the half twist. We get the dividing curves (using the same process as above) connecting the two boundary components with boundary slopes 1. After the section change, we get the dividing curve configuration as shown in Figure 24 at the bottom. Hence one can get the top right dividing curve configuration from the top left dividing curve configuration by section change on the $X \times S^1$. Hence the top right and the top left dividing curve configurations are two different sections of the same tight contact structure on Y .

We had the upper bound $2s+3$ of potential tight contact structures. By the section change described above, s many tight structures are counted twice: one represented by a section with a positive and

FIGURE 24. Different sections of a tight contact structure on $X \times S^1$.

a negative bypass and the other section with the same signed bypass and half a twist across the incompressible torus. Hence we get a tighter upper bound of $s + 3$. Since $s = \sum_{i=1}^4 \lfloor \frac{q_i}{p_i} \rfloor$ and we get that $s + 3 = |e_0(M) + 1|$. Hence the number of the potential tight contact structures on $X \times S^1$ is bounded above by $|e_0(M) + 1|$.

The solid torus V_i has a boundary slope of $-\frac{q_i - \lfloor \frac{q_i}{p_i} \rfloor p_i}{v_i - \lfloor \frac{q_i}{p_i} \rfloor u_i} = -\frac{q_i + (a_0^i + 1)p_i}{v_i + (a_0^i)u_i}$. With this boundary slope, there are exactly $\prod_{j=1}^m (a_j^i + 1)$ tight contact structures on V_i (Theorem 2.3 in [21]). Thus, up to contact isotopy there are at most $|e_0(M) + 1| \prod_{i=1}^4 \prod_{j=1}^m (a_j^i + 1)$ tight contact structures with zero Giroux torsion on $M = M(0; -q_1/p_1, -q_2/p_2, -q_3/p_3, -q_4/p_4)$ with $e_0(M) \leq -4$.

Since the upper bound and lower bound match, we get $|\pi_0(\text{Tight}^{\text{min}}(M))| = |(e_0(M) + 1) \prod_{i=1}^4 \prod_{j=1}^m (a_j^i + 1)|$. All of these are Stein fillable since we get these contact structures on M by doing a -1 Legendrian surgery on a Legendrian link in (S^3, ξ_{std}) .

Since M is toroidal there are \mathbb{Z} many non-isotopic tight contact structures on M corresponding to integral Giroux torsion. As seen in the example case the tight contact structures on M with non-zero Giroux torsion are not weakly fillable. \square

3.3. Concluding remarks. One can try to classify tight contact structures on Seifert fibered manifold $M = M(0, e_0; p_1/q_1, \dots, p_4/q_4)$ where $e_0 > -4$ and with, $(p_i, q_i) = 1$. We can construct tight contact structures with zero Giroux torsion by Legendrian surgery to get a lower bound on the number of tight contact structures. To get the upper bound on the number of tight contact structures we use convex surface theory. These two bounds don't match. Currently, the author is unable to find any contact

isotopy between the contact structures found by convex surface theory or find an invariant to say that those are non-isotopic contact

REFERENCES

- [1] Daniel Bennequin. Entrelacements et équations de pfaff. *Astérisque*, 107:87, 1983.
- [2] Vincent Colin, Emmanuel Giroux, and Ko Honda. On the coarse classification of tight contact structures. *arXiv preprint math/0305186*, 2003.
- [3] Yakov Eliashberg. Classification of overtwisted contact structures on 3-manifolds. *Inventiones mathematicae*, 98(3):623–637, 1989.
- [4] Yakov Eliashberg. Topological characterization of stein manifolds of dimension > 2 . *International Journal of Mathematics*, 01(01):29–46, 1990.
- [5] Yakov Eliashberg. Contact 3-manifolds twenty years since j. martinet’s work. In *Annales de l’institut Fourier*, volume 42, pages 165–192, 1992.
- [6] Yakov Eliashberg and Mikhael Gromov. Convex symplectic manifolds. *Several complex variables and complex geometry*, pages 135–162, 1991.
- [7] John B. Etnyre. Introductory lectures on contact geometry, 2002.
- [8] John B Etnyre. Convex surfaces in contact geometry: class notes. *Lecture notes available on: <http://people.math.gatech.edu/~etnyre/preprints/papers/surfaces.pdf>*, 2004.
- [9] John B. Etnyre and Ko Honda. On connected sums and Legendrian knots. *Adv. Math.*, 179(1):59–74, 2003.
- [10] David T Gay. Four-dimensional symplectic cobordisms containing three-handles. *Geometry & Topology*, 10(3):1749–1759, 2006.
- [11] Hansjörg Geiges. *An introduction to contact topology*, volume 109 of *Cambridge Studies in Advanced Mathematics*. Cambridge University Press, Cambridge, 2008.
- [12] Paolo Ghiggini. On tight contact structures with negative maximal twisting number on small seifert manifolds, 2007.
- [13] Paolo Ghiggini and Ko Honda. Giroux torsion and twisted coefficients. *arXiv preprint arXiv:0804.1568*, 2008.
- [14] Paolo Ghiggini, Paolo Lisca, and András Stipsicz. Tight contact structures on some small seifert fibered 3-manifolds. *American journal of mathematics*, 129(5):1403–1447, 2007.
- [15] Paolo Ghiggini, Paolo Lisca, and András I Stipsicz. Classification of tight contact structures on small seifert 3-manifolds with. *Proceedings of the American Mathematical Society*, pages 909–916, 2006.
- [16] Paolo Ghiggini and Stephan Schönenberger. On the classification of tight contact structures. *arXiv preprint math/0201099*, 2002.
- [17] Emmanuel Giroux. Convexity in contact topology. *Comment. Math. Helv*, 66(4):637–677, 1991.
- [18] Emmanuel Giroux. Géométrie de contact: de la dimension trois vers les dimensions supérieures. *arXiv preprint math/0305129*, 2003.
- [19] Robert E. Gompf. Handlebody construction of stein surfaces, 1998.
- [20] Allen Hatcher. Notes on basic 3-manifold topology, 2007.
- [21] Ko Honda. On the classification of tight contact structures i. *arXiv preprint math/9910127*, 1999.
- [22] Ko Honda. On the classification of tight contact structures ii. *Journal of Differential Geometry*, 55(1):83–143, 2000.
- [23] Ko Honda. Notes for math 599: contact geometry. *Lecture Notes available at <http://www-bcf.usc.edu/~khonda/math599/notes.pdf>*, 2019.
- [24] Ko Honda, William H Kazez, and Gordana Matić. Convex decomposition theory. *International Mathematics Research Notices*, 2002(2):55–88, 2002.
- [25] P Lisca and G Matić. Tight contact structures and Seiberg-Witten invariants. *Invent. Math.*, 129(3):509–525, aug 1997.
- [26] Paolo Lisca and G Matić. Stein 4-manifolds with boundary and contact structures. *Topology and its Applications*, 88(1-2):55–66, 1998.
- [27] Paolo Lisca and András I Stipsicz. Ozsváth-szabó invariants and tight contact 3-manifolds, iii. *JOURNAL OF SYMPLECTIC GEOMETRY*, 2007.
- [28] Jean Martinet. Formes de contact sur les variétés de dimension 3. In *Proceedings of Liverpool Singularities Symposium II*, pages 142–163. Springer, 2006.

- [29] Irena Matkovic. Classification of tight contact structures on small seifert fibered l-spaces. *Algebr. Geom. Topol.*, 18(1):111–152, 2018.
- [30] Jonathan Simone. Tight contact structures on some plumbed 3-manifolds. *arXiv preprint arXiv:1710.06702*, 2017.
- [31] Andy Wand. Tightness is preserved by legendrian surgery. *Annals of Mathematics*, pages 723–738, 2015.
- [32] Hao Wu. *Tight contact structures on small Seifert spaces*. PhD thesis, Massachusetts Institute of Technology, 2004.
- [33] Kanda Yutaka. The classification of tight contact structures on the 3-torus. *Communications in Analysis and Geometry*, 5(3):413–438, 1997.

Tanushree Shah
tanushrees@cmi.ac.in
Chennai Mathematical Institute